Tetraarylpyrrolo[3,2-*b*]pyrroles as versatile and responsive fluorescent linkers in Metal-Organic Frameworks

Chris S. Hawes,*[a,b] Gearóid M. Ó Máille,[b] Kevin Byrne,[c] Wolfgang Schmitt[c] and Thorfinnur Gunnlaugsson*[b]

a. School of Chemical and Physical Sciences, Keele University, Keele ST5 5BG, United Kingdom

b. School of Chemistry and Trinity Biomedical Sciences Institute, The University of Dublin, Trinity College Dublin, Dublin 2, Ireland

c. School of Chemistry and Centre for Research on Adaptive Nanostructures and Nanodevices, The University of Dublin, Trinity College Dublin, Dublin 2, Ireland

Supporting Information

1. X-ray powder diffraction data 2
2. Thermogravimetric analysis 5
3. Spectroscopic data 7
4. Gas adsorption data 12
5. NMR spectra 15
6. References 22

1. X-ray Powder Diffraction Data

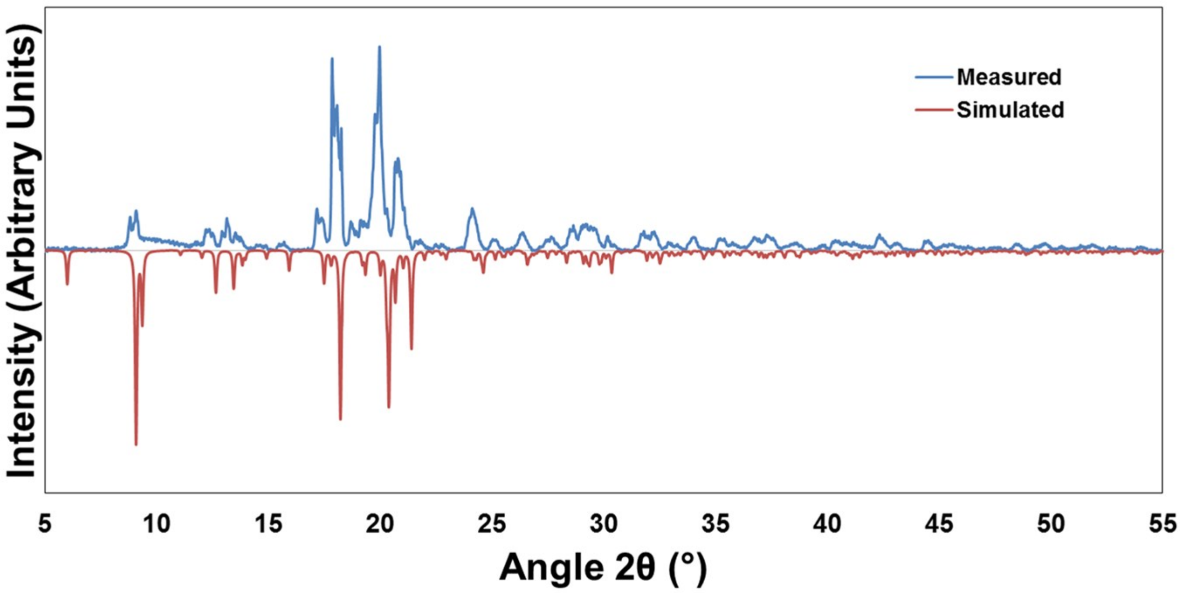

Figure S1 X-ray powder diffraction pattern for complex **1** (blue, room temperature) compared with the pattern simulated from single crystal diffraction data (red, 100 K)

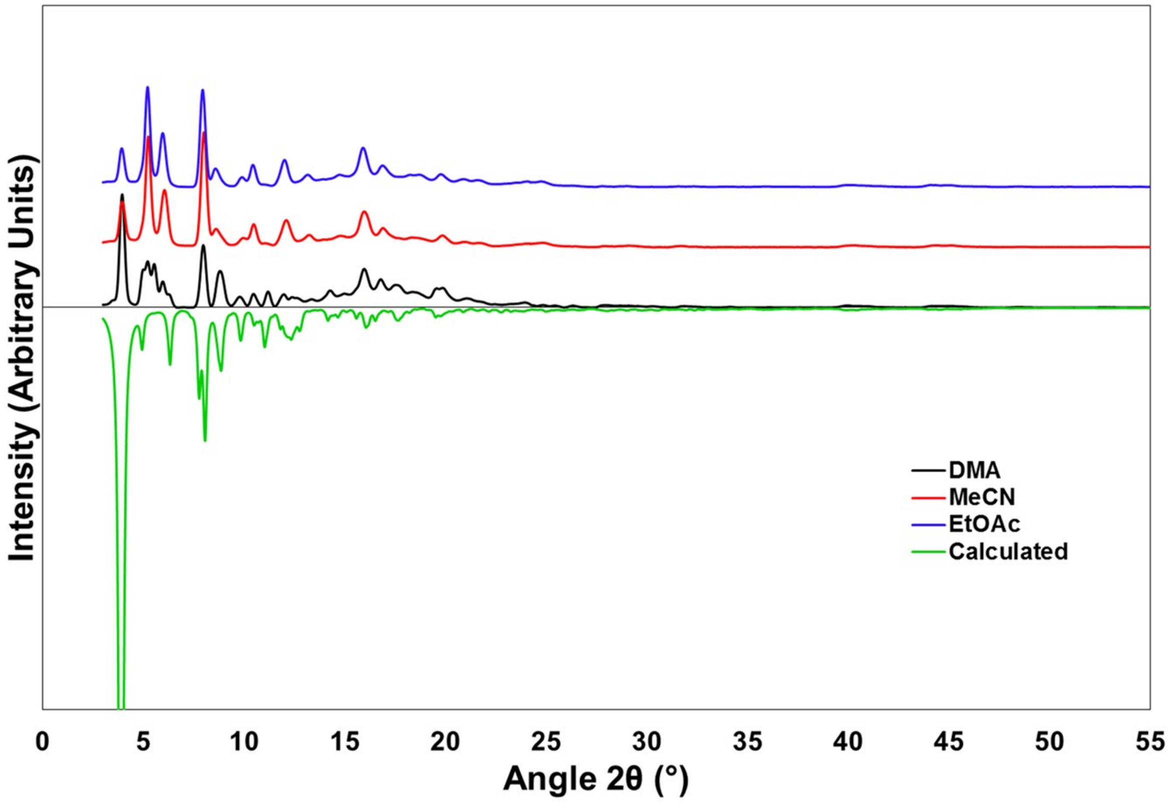

Figure S2 X-ray powder diffraction patterns for complex **2** with guest solvents DMA (Black), MeCN (red) and EtOAc (blue), all measured at 100 K, compared with the pattern simulated from single crystal diffraction data (green). The simulated pattern is modelled at FWHM = 0.2° to better simulate the loss of angular resolution from measuring and integrating Debye rings using an area detector.

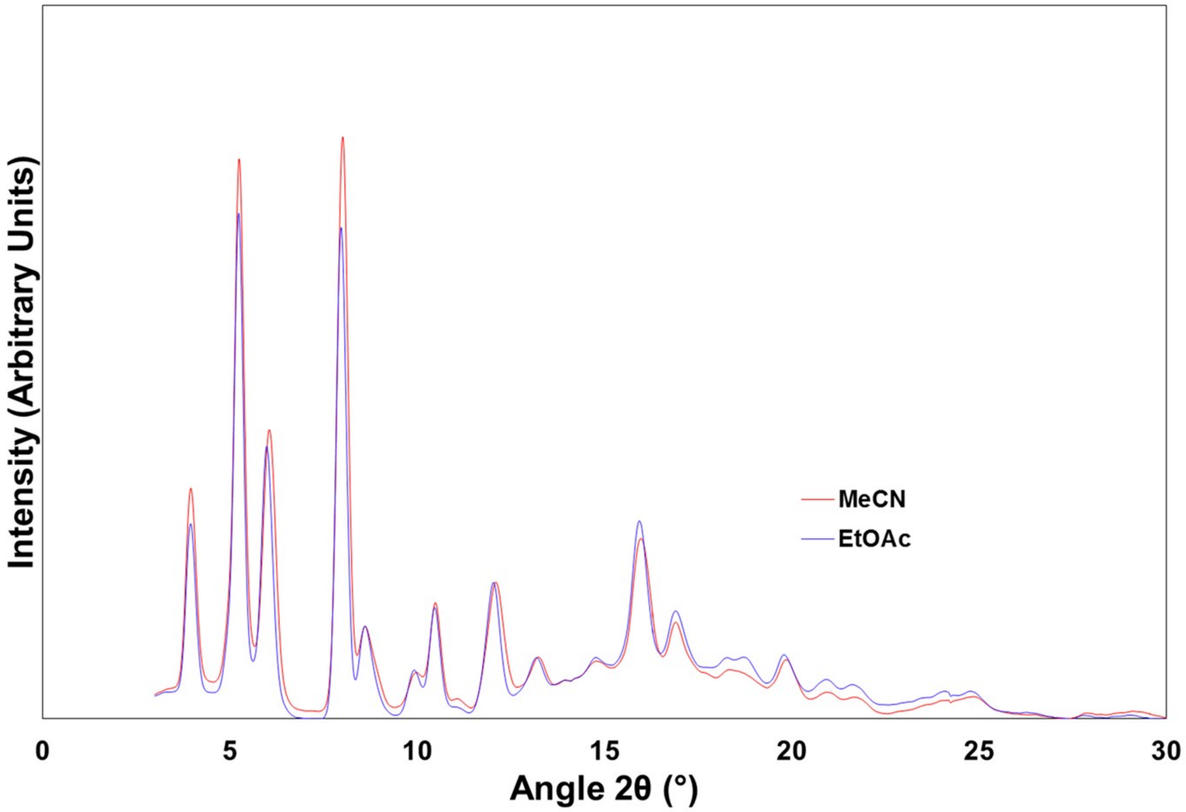

Figure S3 Enlargement of the X-ray powder diffraction patterns in the 2θ = 3-30 ° region showing the similarity between the MeCN and EtOAc soaked complex **2** samples.

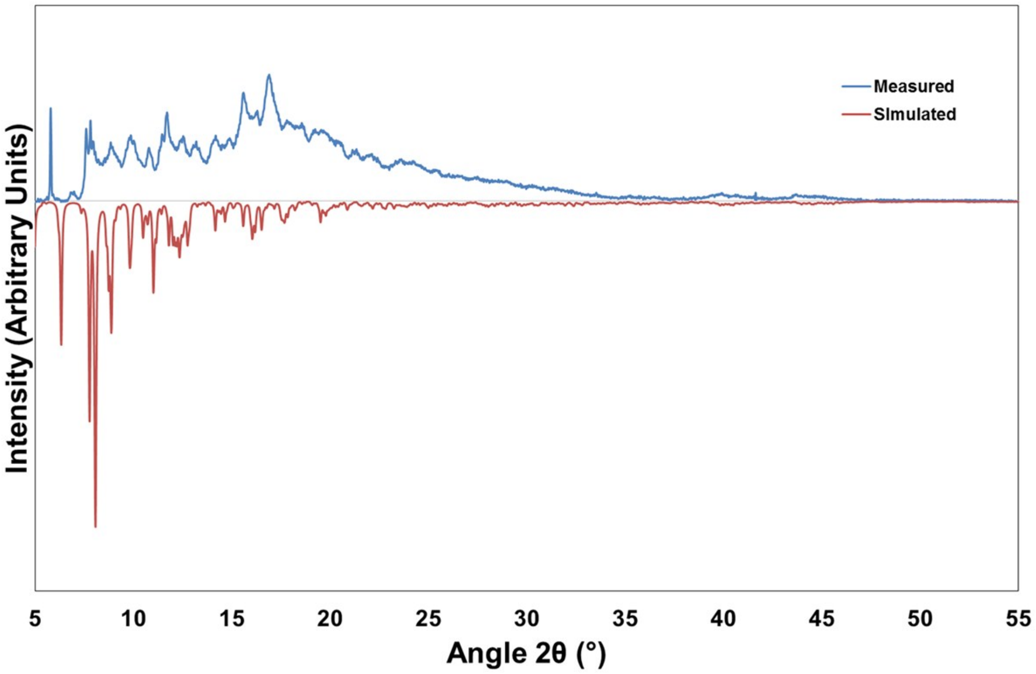

Figure S4 X-ray powder diffraction pattern of air-exposed complex **2** (blue, room temperature) compared with the pattern simulated from single crystal data (red, 100 K).

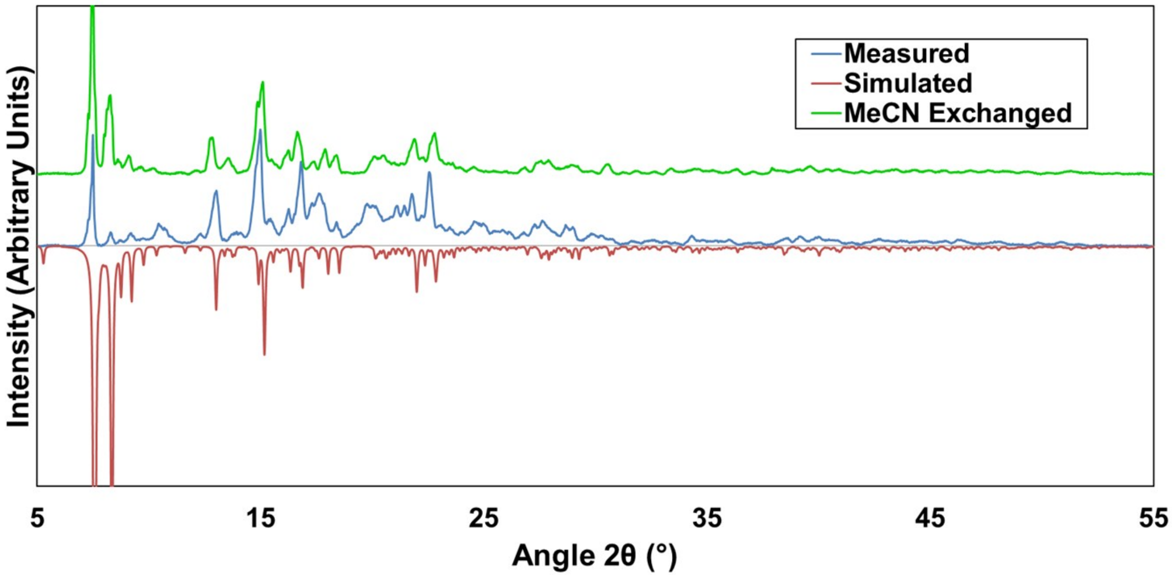

Figure S5 X-ray powder diffraction pattern for complex **3** (blue, room temperature) compared to the pattern simulated from single-crystal data (red, 100 K), and the pattern observed from the MeCN-exchanged and air-exposed material (green, room temperature).

2. Thermogravimetric Analysis

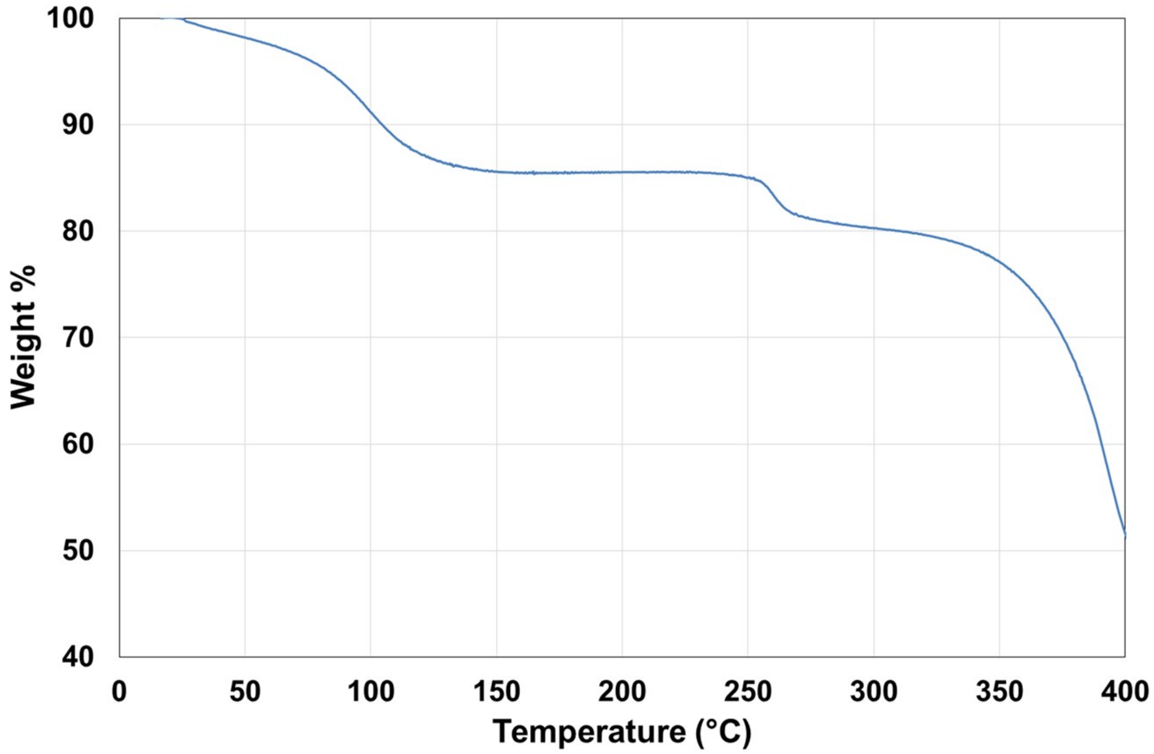

Figure S6 Thermogravimetric analysis plot for complex **1**

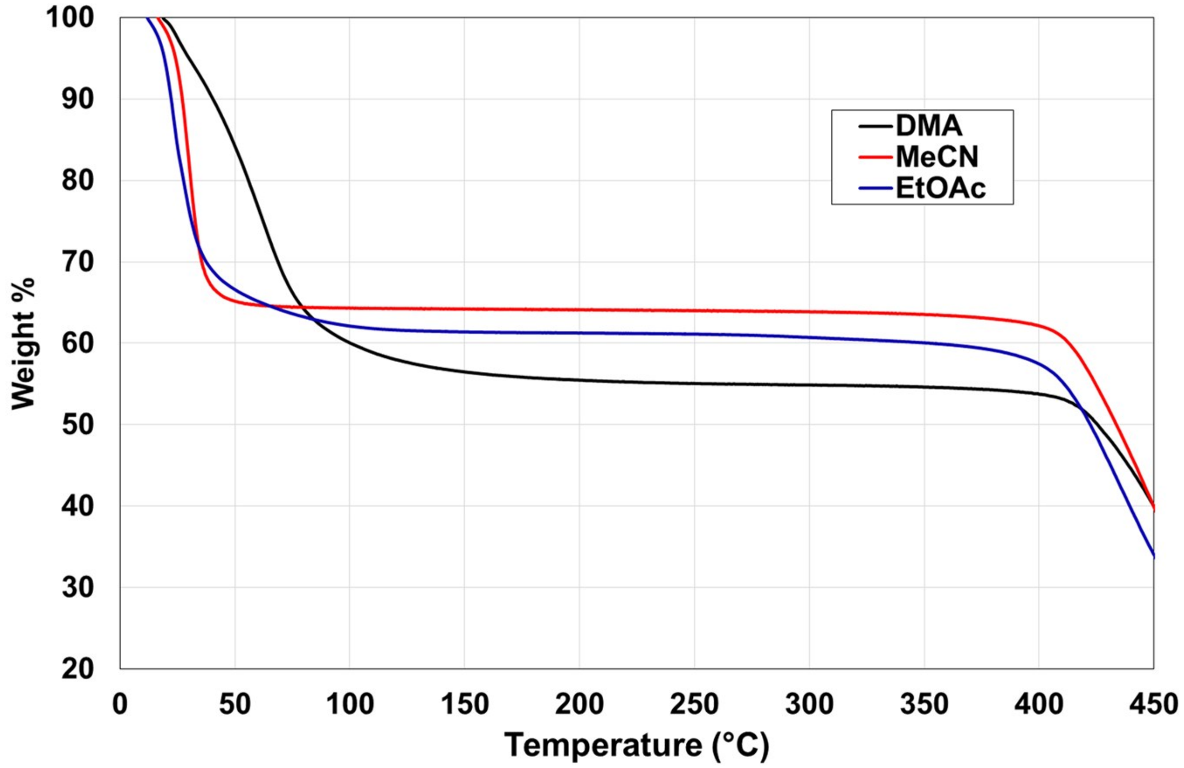

Figure S7 Thermogravimetric analysis plot for complex **2** with DMA (black), MeCN (red) and EtOAc (blue) guests.

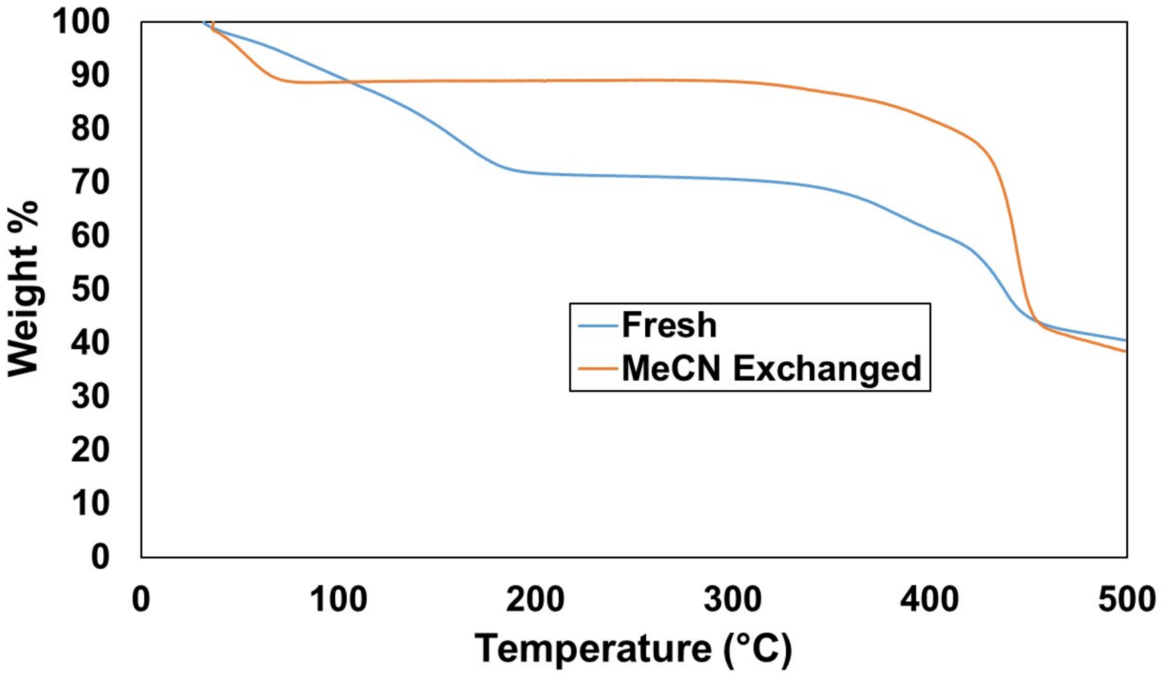

Figure S8 Thermogravimetric analysis plot for complex **3**, freshly prepared (blue) and following exchange with MeCN (orange).

3. Spectroscopic Data

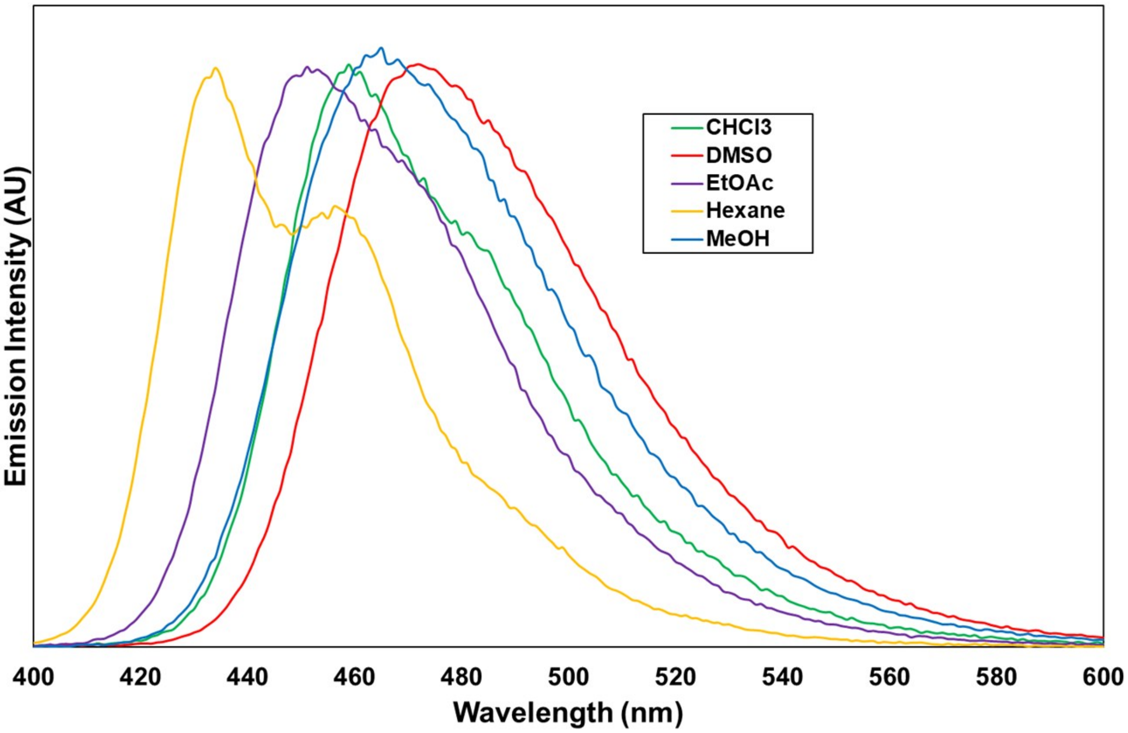

Figure S9 Normalised emission spectra (λ_{ex} = 366 nm, c = 14 μM) for **L1** in various solvents.

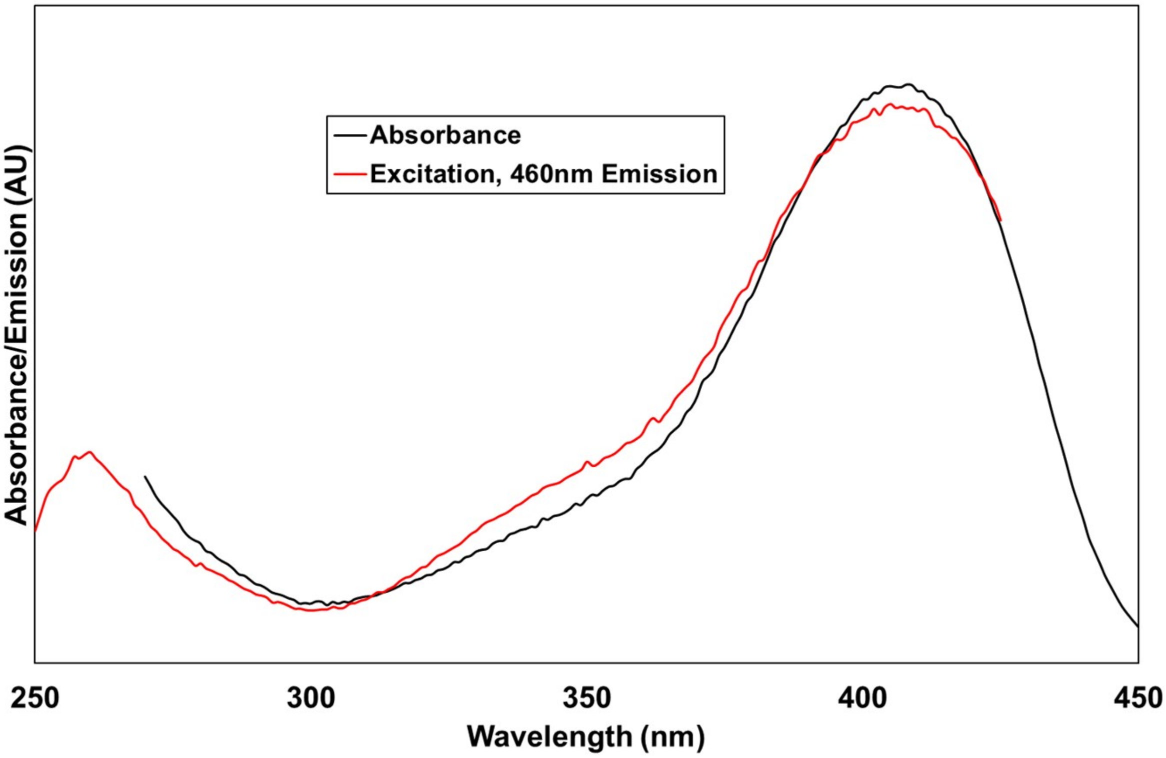

Figure S10 Overlay of absorption and excitation spectra (λ_{em} = 460 nm) for **L1** in $CHCl_3$ (c = 2.5 μM)

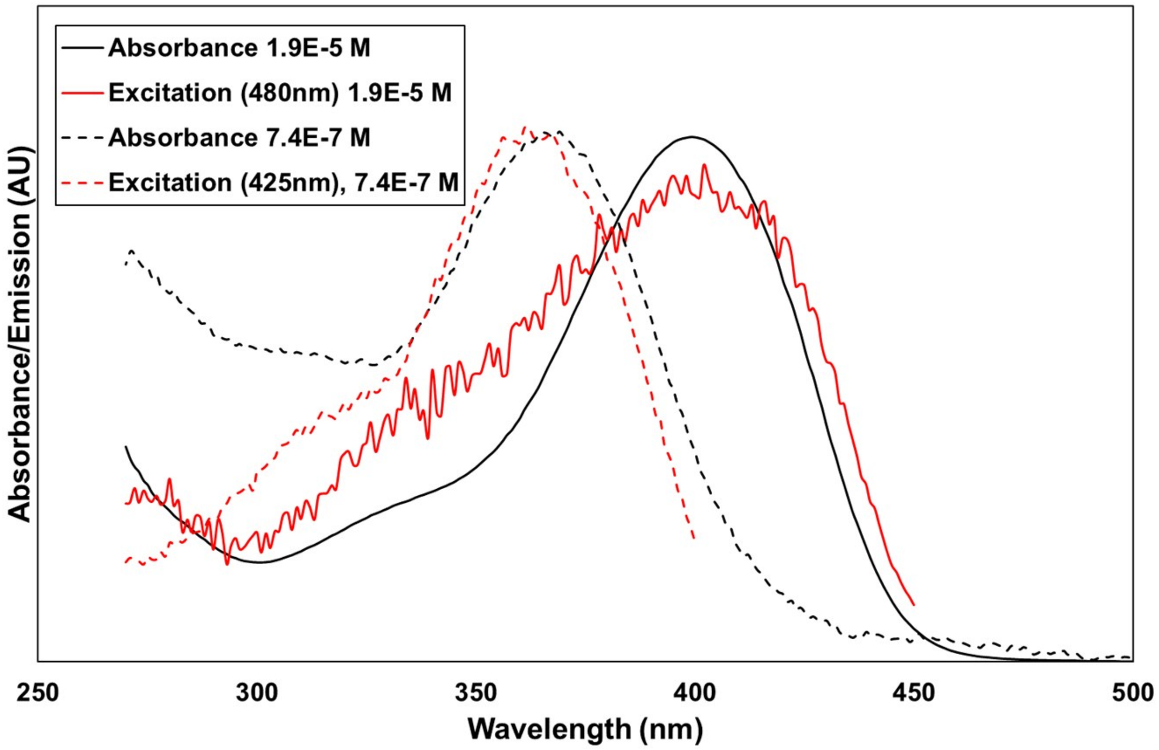

Figure S11 Overlay of absorption (black) and excitation (red) spectra for **H_2L2** in low-concentration and high-concentration states. Excitation spectra are measured for λ_{em} at the given concentrations.

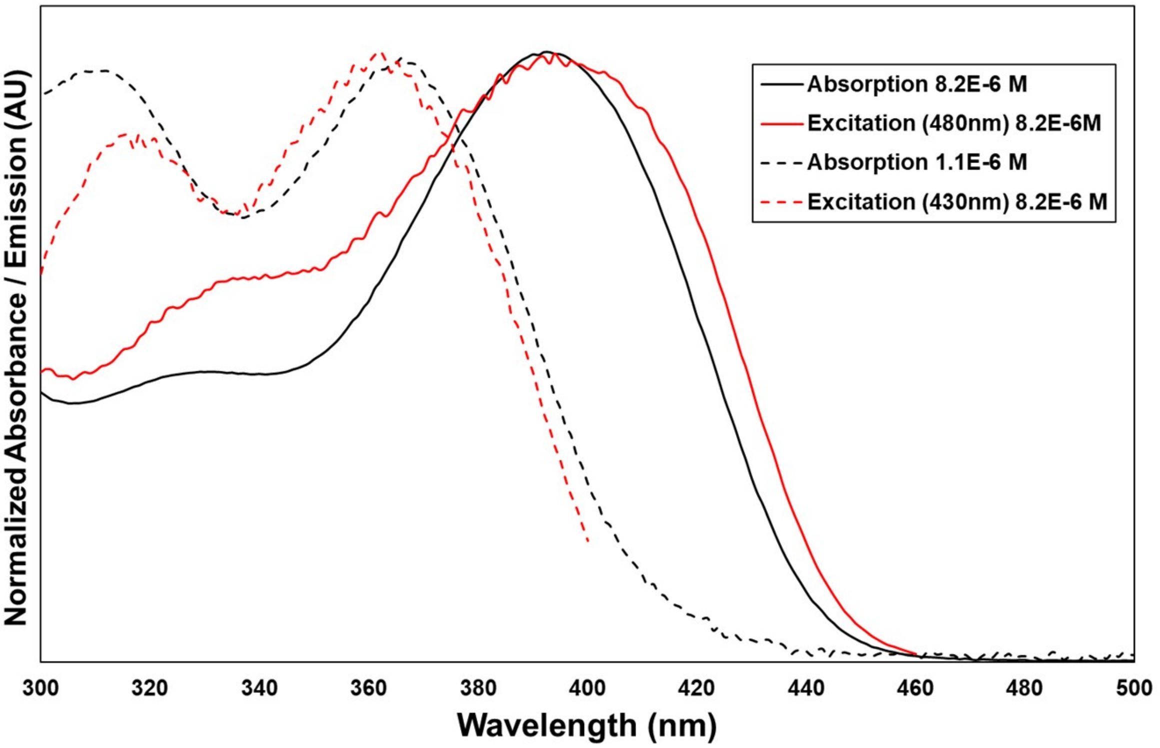

Figure S12 Overlaid absorption (black) and excitation (red) spectra for **H_2L3** in the low and high concentration states.

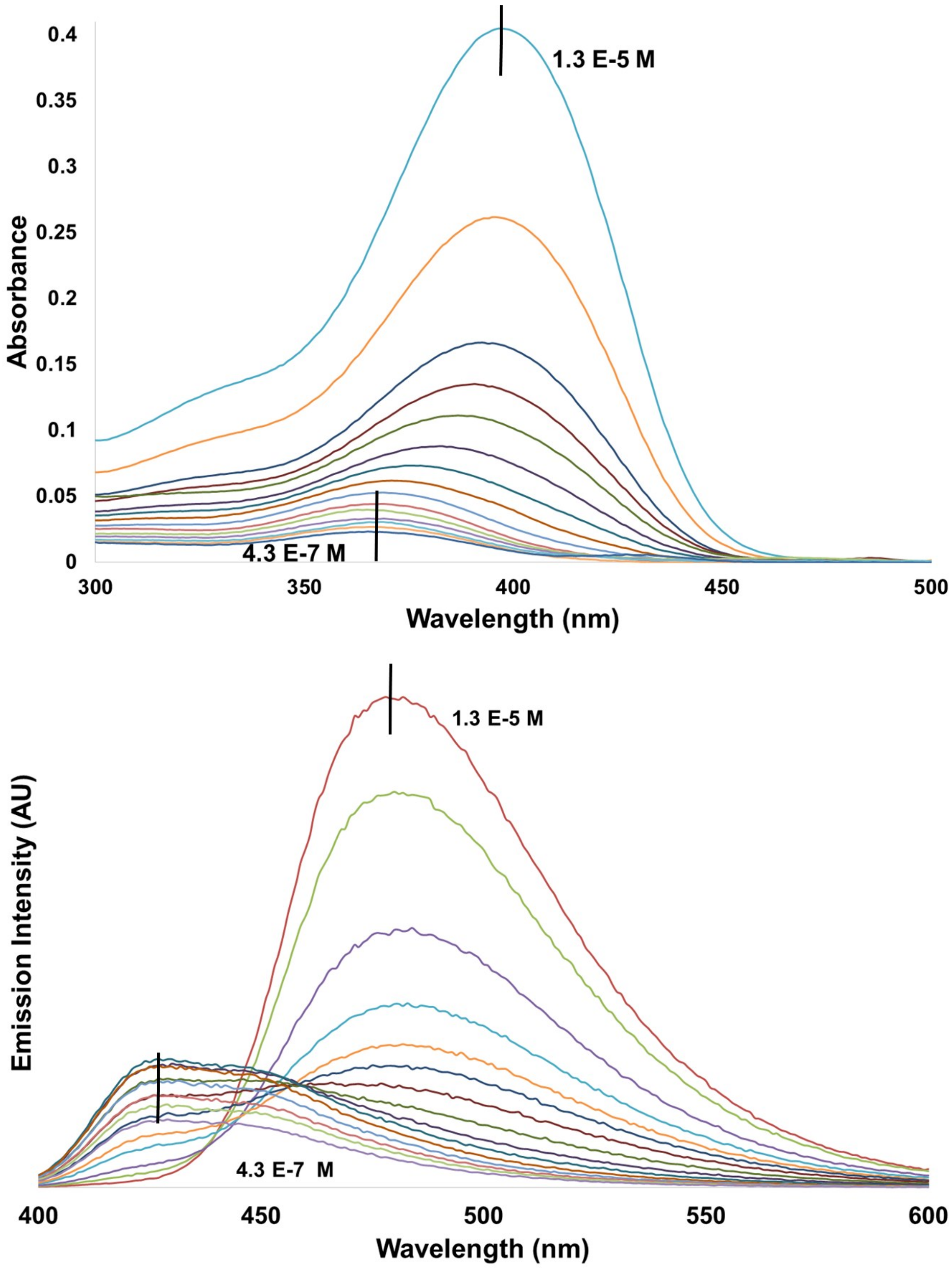

Figure S13 Overlay of sequential dilutions of a solution of **H_2L2** (13 μM) in DMSO, showing the concentration dependence on the absorbance (top) and emission profiles (bottom, λ_{ex} = 366 nm). Absorbance or emission band maxima are indicated with black lines to aid visualisation.

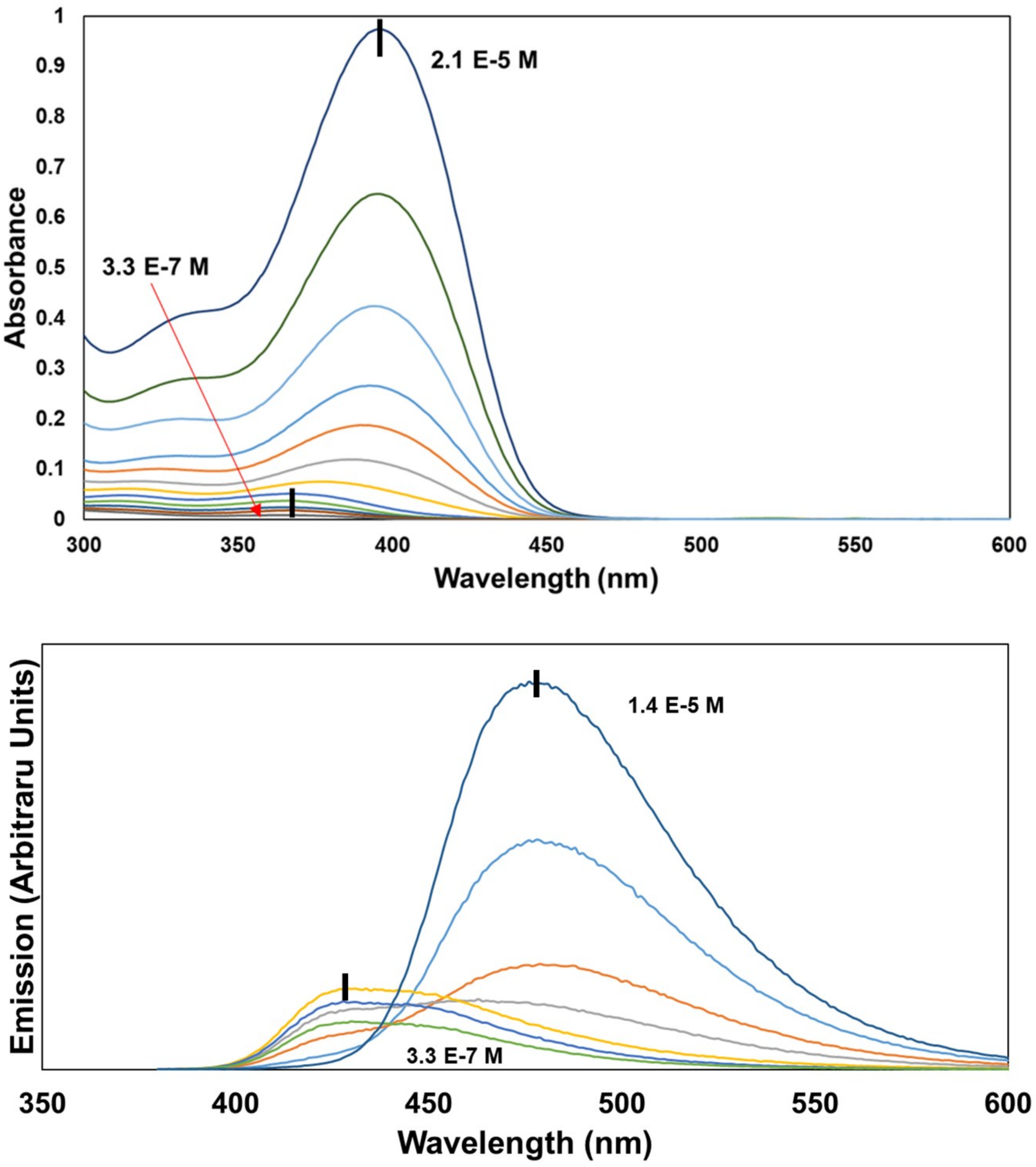

Figure S14 Overlay of sequential dilutions of a solution of **H_2L3** in DMSO, showing the effect on absorption (top) and emission (bottom, λ_{ex} = 366 nm). Black lines added to aid visualisation of the peak maxima.

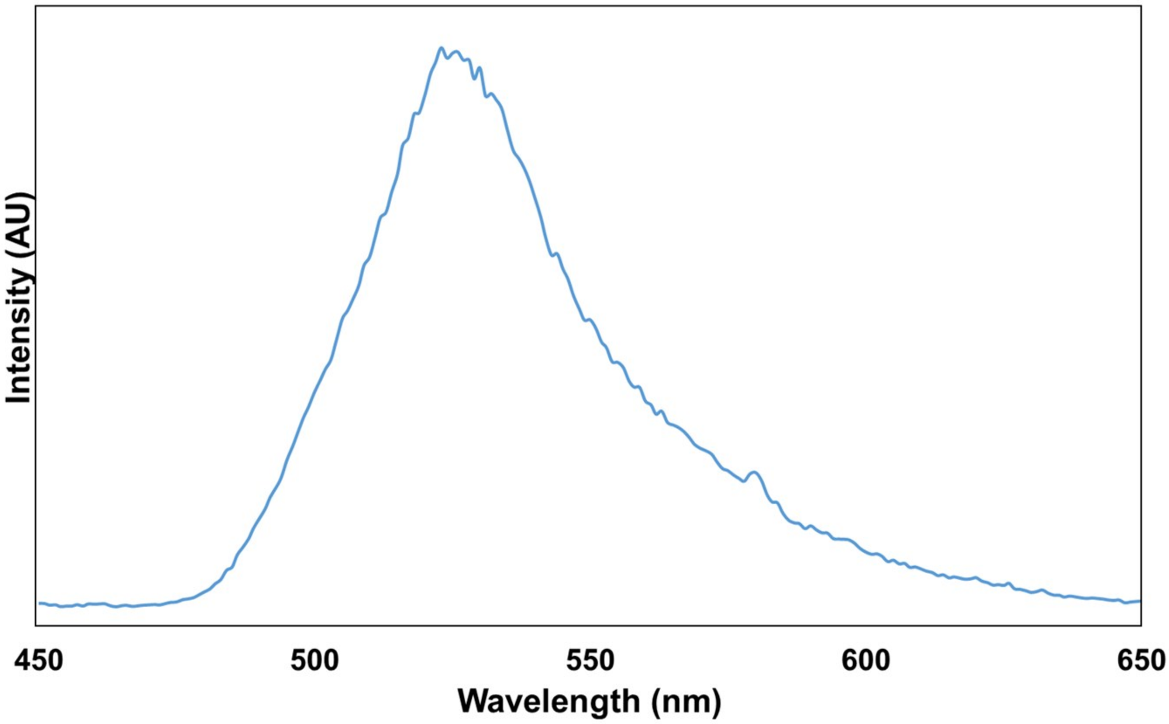

Figure S15 Solid-state emission spectrum (λ_{ex} = 366 nm) for complex **1**.

Quantum Yield Determinations

Photoluminescence quantum yields were determined by the comparative method,[S1] using quinine sulfate in 2M sulfuric acid as a reference ($\Phi = 0.546$).[S2] The absorbance at 366 nm and emission, integrated across the range 380 – 600 nm (excitation & emission slit widths 2.5 nm), were measured across a range of concentrations and plotted, and the quantum yield of the unknown was given by the following relation, where η is the refractive index of each solvent.

$$\Phi_{unknown} = \Phi_{standard}(Grad_{unknown}/Grad_{standard})(\eta^2_{standard}/\eta^2_{unknown})$$

Each series of measurements was carried out in duplicate and the final values averaged, giving agreement within the accepted margin of error of ± 10%. In the cases of **H_2L2** and **H2L3** in DMSO, the high-concentration forms did not return a linear relationship between absorbance and integrated emission intensity at concentrations where the low-concentration form was not present (i.e. above 5 µM, where $A > 0.2$), and so Φ_{PL} was not determined.

4. Gas Adsorption Data

BET Surface Area Calculations

Complex 2: Datapoints for BET surface area calculation were taken from the desorption branch from the 77 K isotherm.

Relative Pressure	Volume @ STP	1 / [W((Po/P) - 1)]
1.98E-01	202.1495	9.77E-01
1.49E-01	194.7172	7.17E-01
1.01E-01	185.5622	4.83E-01
5.25E-02	172.7989	2.57E-01
9.94E-03	140.5102	5.71E-02
7.64E-03	136.6504	4.51E-02
5.32E-03	131.6596	3.25E-02
BET summary		
Slope = 4.851		
Intercept = 4.672e-03		
Correlation coefficient, r = 0.999782		
C constant = 1039.298		
Surface Area = 717.190 m^2/g		

Complex 3: Datapoints were taken from the adsorption branch at 77K.

Relative Pressure	Volume @ STP	1 / [W((Po/P) - 1)]
9.22E-03	324.0746	2.30E-02
1.02E-02	325.0268	2.53E-02
2.53E-02	337.5448	6.15E-02
4.96E-02	347.4498	1.20E-01
7.43E-02	353.6012	1.82E-01
BET summary		
Slope = 2.433		
Intercept = -2.777e-04		
Correlation coefficient, r = 0.999969		
C constant = 8762.832		
Surface Area = 1431.094 m^2/g		

Isosteric Heat of Adsorption Calculations

The heat of adsorption for CO_2 within complexes **2** and **3** was calculated using least-squares fitting of a virial thermal adsorption equation[S3], which models Ln(P) as a function of gas adsorbed. Datapoints were collected at 273, 283 and 293 K. The model function takes the form $\ln(P) = \{\ln(N) + (a_0 + a_1N + a_2N^2\ldots)/T + b\}$, where N represents the surface excess adsorption (mmol) at temperature T and a_0, a_1 and a_2 are coefficients determined through least-squares fitting. The original parameter set of 5 parameters was sequentially reduced to maximise the data:parameter ratio. The enthalpy of adsorption is then given by the relation $Q(N) = -R(a_0 + a_1N + a_2N^2)$. Optimised coefficients and parameters are given below.

Complex 2:

Temperatures (K)	273, 283, 293
a_0	-2905.92
a_1	154.6669
a_2	-12.1149
B	13.6838
R^2	0.9968
Datapoints fitted	60

Complex 3:

Temperatures (K)	278, 293, 308
a_0	-3082.19
a_1	8.5197
B	13.52901
R^2	0.9853
Datapoints fitted	62

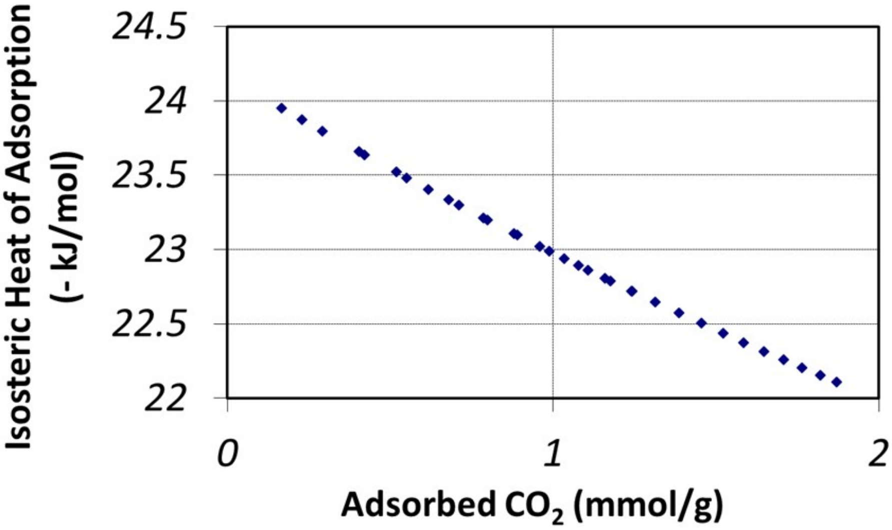

Figure S16 Enthalpy of adsorption estimated as a function of CO_2 loading for complex **2**

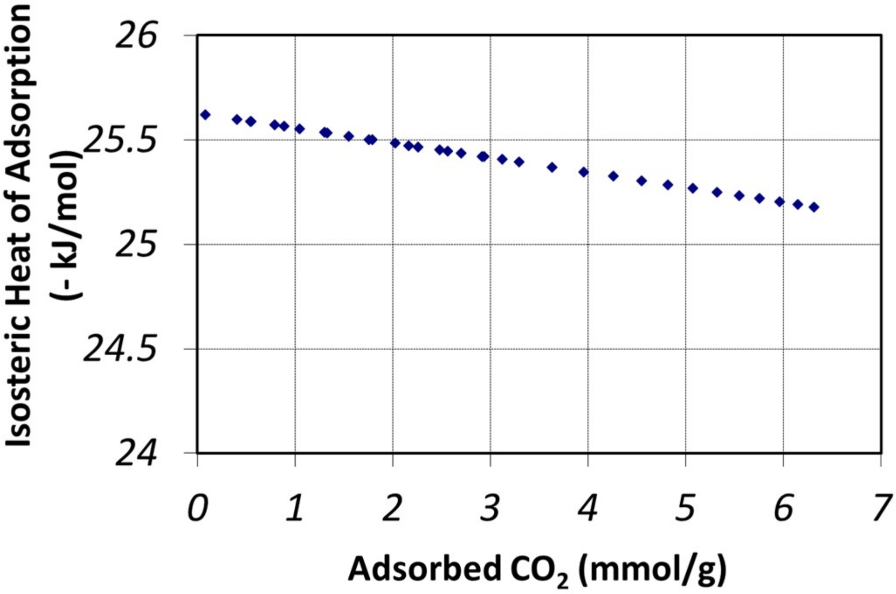

Figure S17 Enthalpy of adsorption estimated as a function of CO_2 loading for complex **3**

5. NMR Spectra

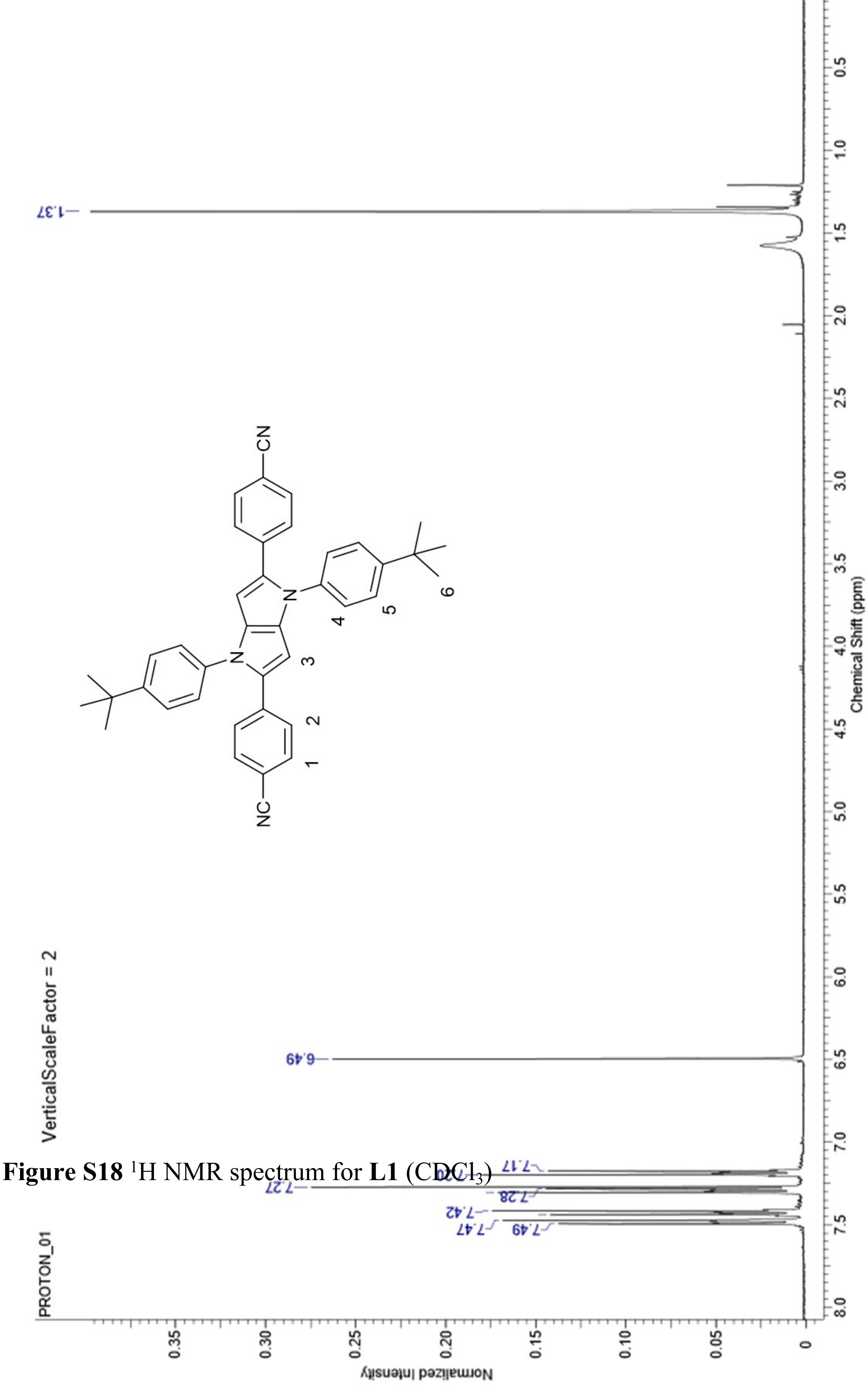

Figure S18 ^{1}H NMR spectrum for **L1** ($CDCl_3$)

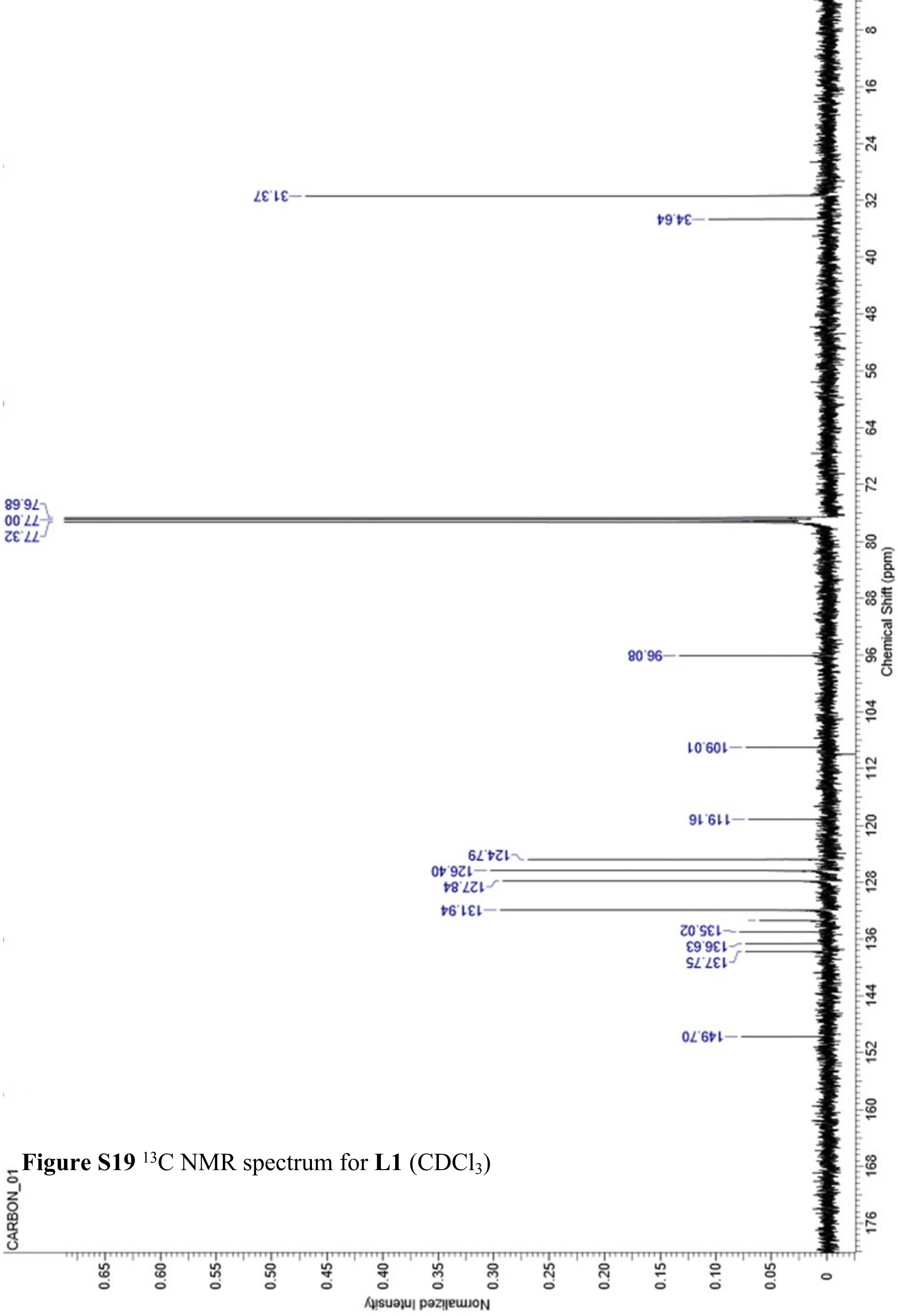

Figure S19 ^{13}C NMR spectrum for **L1** ($CDCl_3$)

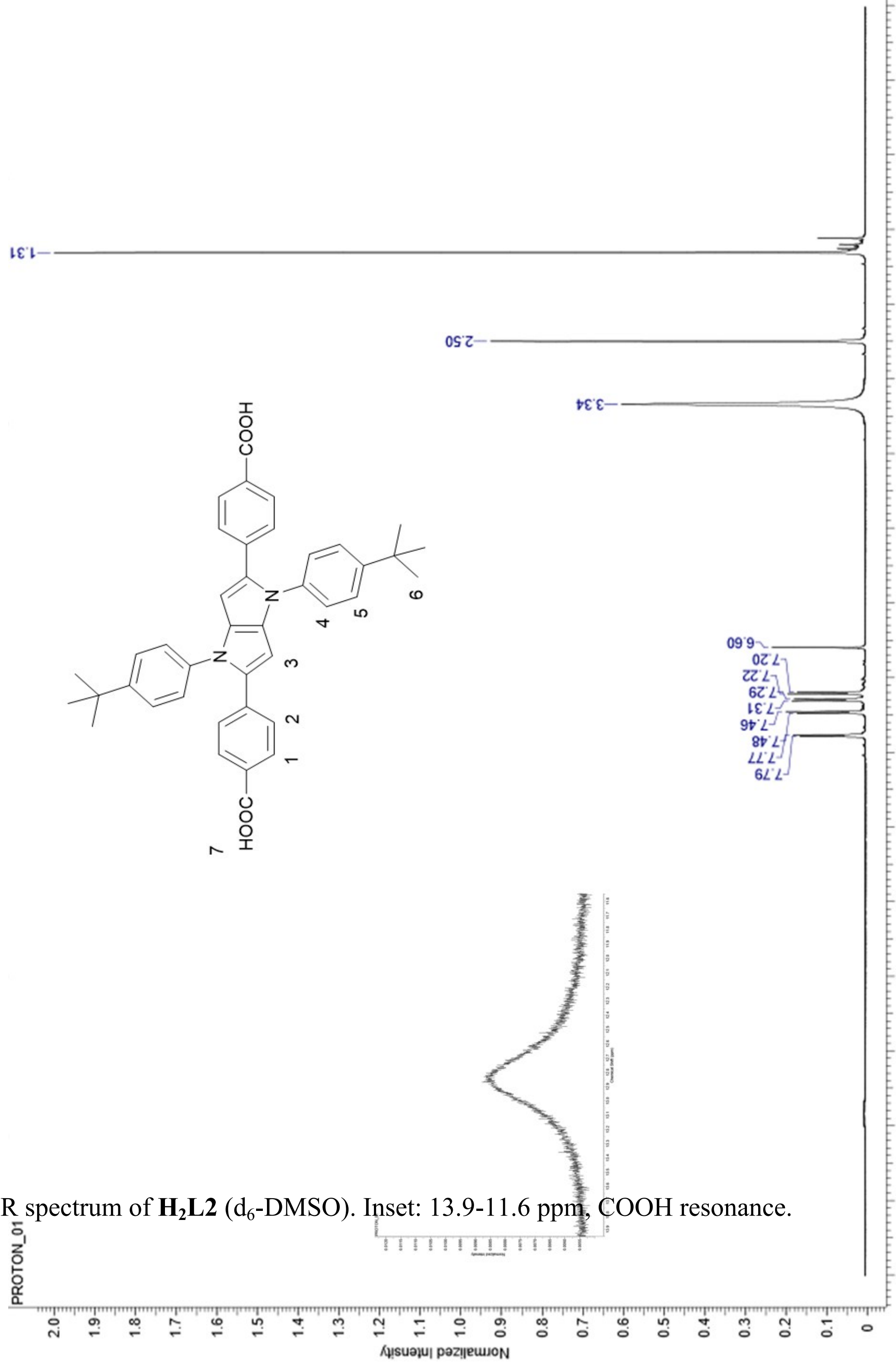

Figure S20 ^{1}H NMR spectrum of **H_2L2** (d_6-DMSO). Inset: 13.9-11.6 ppm, COOH resonance.

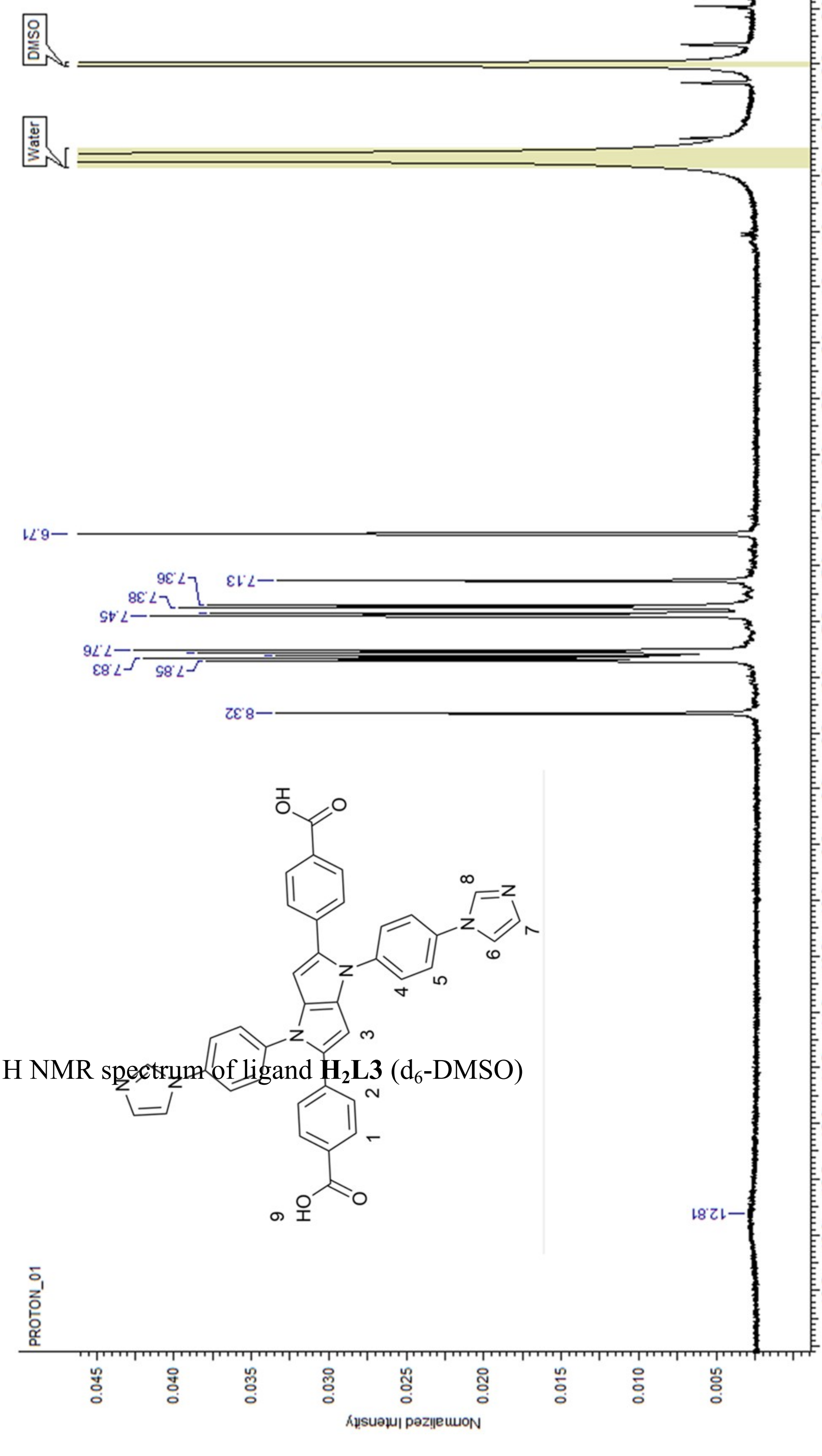

Figure S21 ^{1}H NMR spectrum of ligand **H_2L3** (d_6-DMSO)

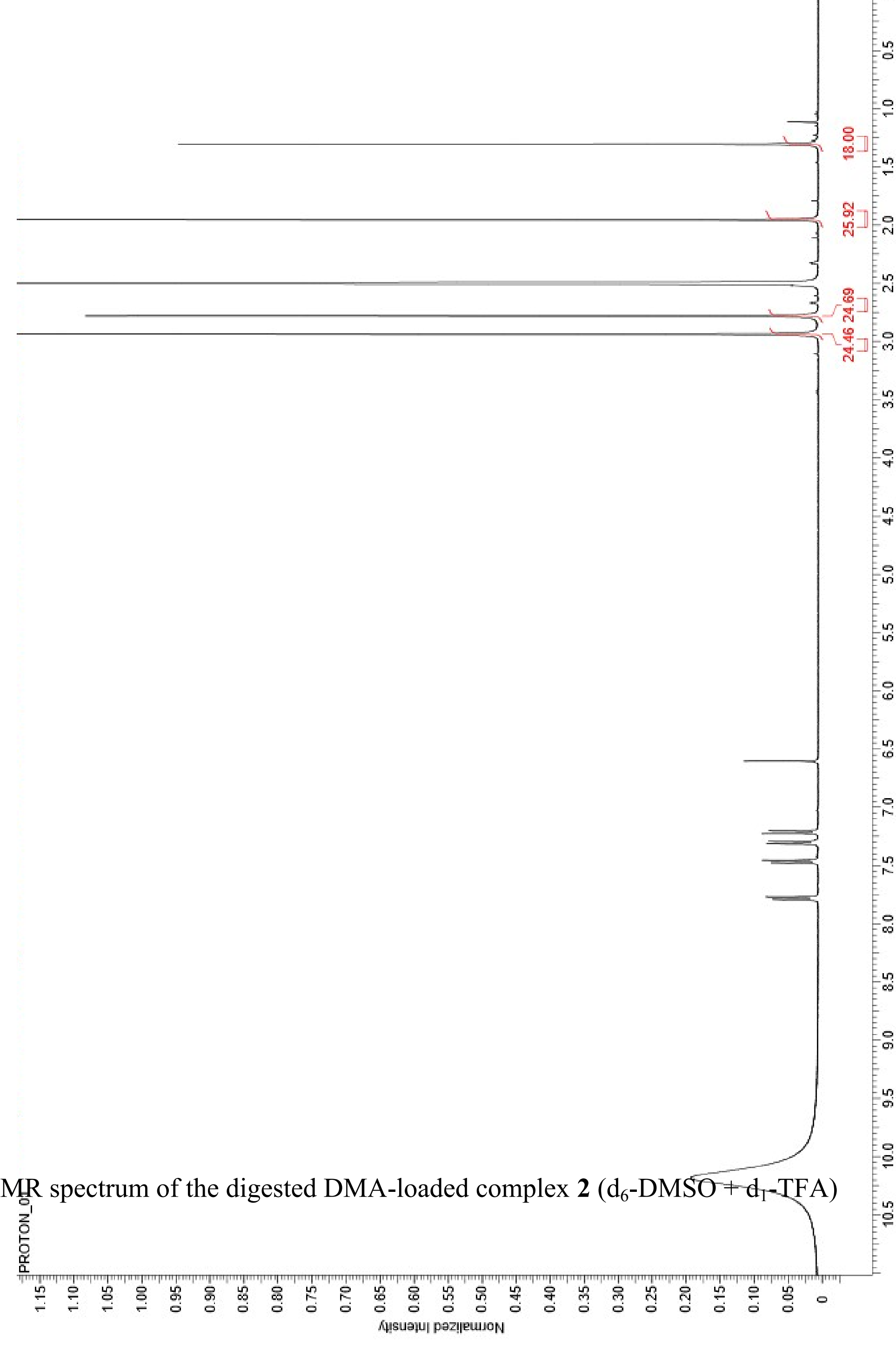

Figure S20: ^{1}H NMR spectrum of the digested DMA-loaded complex **2** (d_6-DMSO + d_1-TFA)

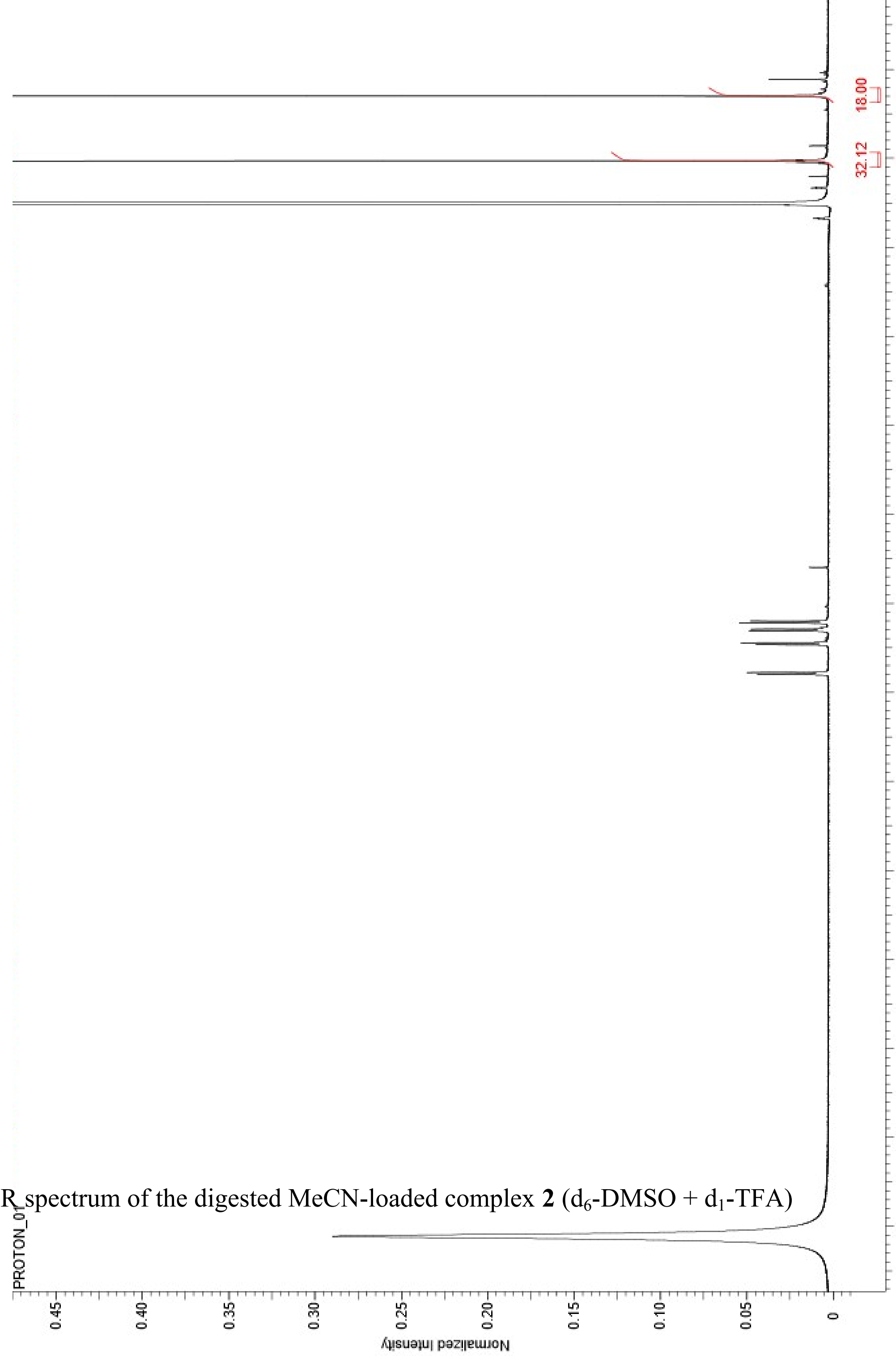

Figure S21: ^{1}H NMR spectrum of the digested MeCN-loaded complex **2** (d_6-DMSO + d_1-TFA)

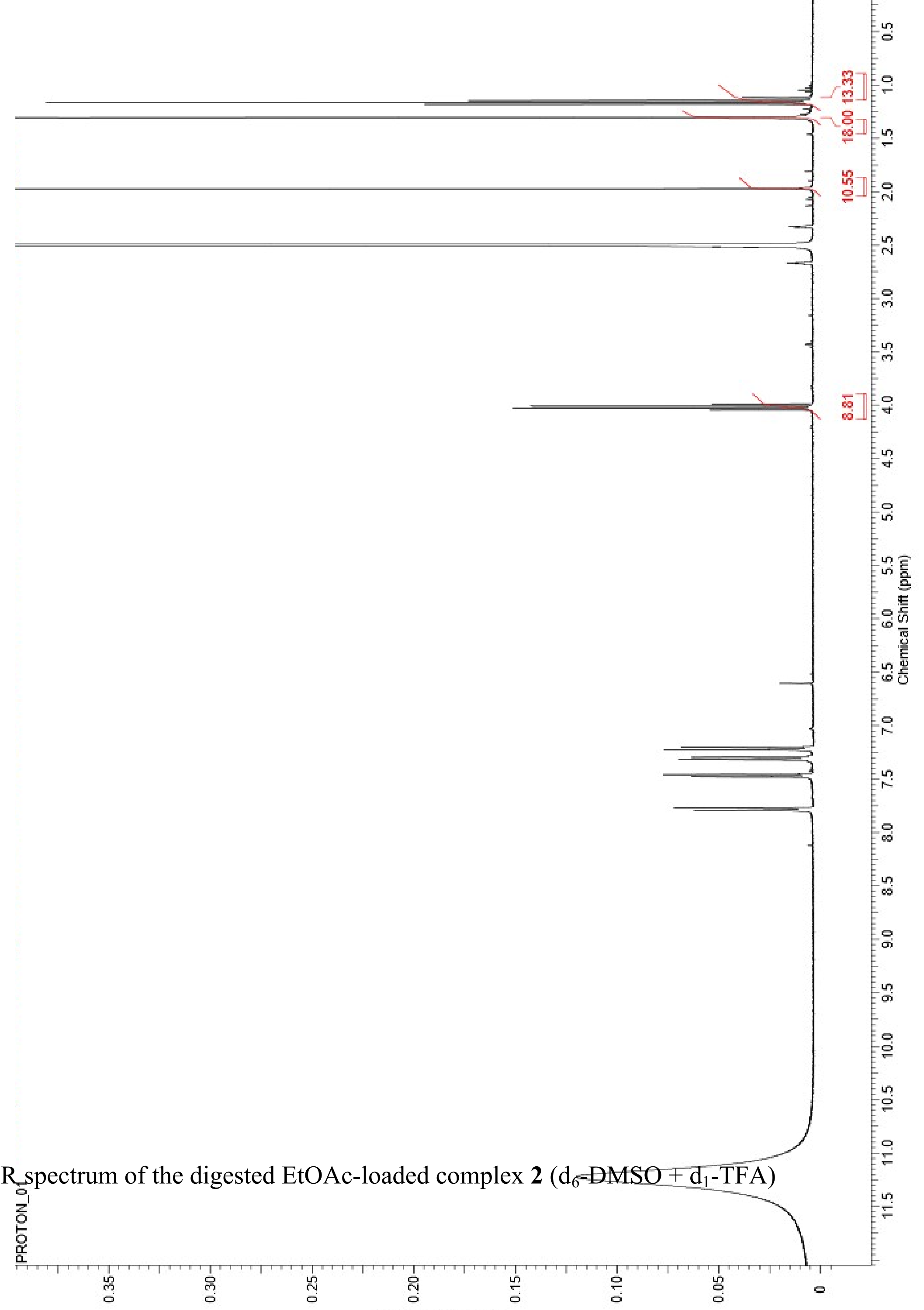

Figure S22: ^{1}H NMR spectrum of the digested EtOAc-loaded complex **2** (d_6-DMSO + d_1-TFA)

6. References

S1 Horiba Scientific, “A Guide to Recording Fluorescence Quantum Yields”, http://www.horiba.com/scientific/products/fluorescence-spectroscopy/application-notes/quantum-yields/; accessed 7/8/2016

S2 Brouwer, A. M.; Standards for photoluminescence quantum yield measurements in solution (IUPAC Technical Report), *Pure Appl. Chem.* **2011**, *83*, 2213-2228

S3 Czepirski, L.; Jagiello, J.; Virial-type thermal equation of gas—solid adsorption, *Chem. Eng. Sci.* **1989**, *44*, 797-801; Tedds, S.; Walton, A.; Broom, D. P.; Book, D.; Characterisation of porous hydrogen storage materials: carbons, zeolites, MOFs and PIMs, *Faraday Discuss.* 2011, **151**, 75-94.